DROUGHT CHARACTERISTICS AND FUTURE SCENARIO PROJECTIONS IN THE MINJIANG RIVER BASIN, CHINA

ZHANG, B.[1] – XIAO, X.[2*] – YANG, C. Z.[1] – LI, X. J.[1] – LI, X. Y.[1]

[1]*Civil Aviation Flight University of China, Chengdu 641419, Sichuan, China*

[2]*Chengdu Meteorological Bureau, Chengdu 611000, Sichuan, China*

**Corresponding author*
e-mail: 240835712@qq.com

(Received 18th Sep 2025; accepted 5th Dec 2025)

Abstract. This study evaluates drought risk in the Minjiang River Basin in Southwest China using daily precipitation records from 1961 to 2022. A multiscale analysis is conducted using the standardized precipitation indices (SPI3 and SPI12), which are validated against recorded drought events. Future drought characteristics are further assessed under multiple emission scenarios. Results show that, when SPI3 and SPI12 are used jointly, the overall identification rate of historical droughts reaches 78.12%, and 91% for severe and extreme events. Annually, a modest moistening tendency is observed (0.01 per decade), with a more pronounced increase in spring (0.2 per decade), alongside subtle drying during summer, autumn, and winter. Seasonal patterns vary: spring is mainly characterized by mild drought, while the other seasons are characterized by moderate to severe droughts, often accompanied by extreme weather conditions. Spatial hotspots form in Chengdu–Guoluo (spring), Leshan–Ya'an–Aba–Ganzi (summer), Chengdu–Ya'an–Leshan–Zigong–Neijiang (autumn), and Guoluo (winter). Coupled Model Intercomparison Project Phase 6 (CMIP6) multi-model projections reveal divergent drought trajectories under varying emission scenarios: Shared Socioeconomic Pathways scenarios 585 (SSP5-8.5), SSP3-7.0, SSP2-4.5, and SSP1-2.6. With increasing emissions, drought frequency tends to rise and high-risk areas shift from the central basin toward the south and northwest, while the overall affected area decreases. These findings provide a basis for improved monitoring, forecasting, and risk reduction in the basin.
Keywords: *standardized precipitation index, CMIP6, Taylor diagram, multi-model ensemble*

Introduction

Drought is among the most pervasive natural hazards globally, characterized by prolonged duration, broad impacts, and uneven spatiotemporal distribution. It threatens ecosystems, agricultural production, and socioeconomic development (Zhang et al., 2017; Zhai and Zou, 2005). Globally, direct economic losses from drought are estimated at up to USD 8 billion per year, exceeding losses from many other natural disasters (Chen et al., 2023). Drought is commonly classified into meteorological, agricultural, hydrological, and socioeconomic types, with meteorological drought serving as the basis for subsequent categories (Yin and Bai, 2025). Accurate characterization of spatiotemporal patterns underpins drought prevention, mitigation, governance, and sustainable water-resources management. Index-based drought quantification and analysis are now widely applied. Common indices include the Standardized Precipitation Index (SPI), Palmer Drought Severity Index (PDSI), and Standardized Precipitation Evapotranspiration Index (SPEI), which incorporates both precipitation and potential evapotranspiration (Wang et al., 2021). Among these indices, the SPI proposed by McKee et al. (1993) is particularly prominent. Its computational simplicity, modest data requirements, and ability to reveal distributional differences across space and time make it an effective tool across regional and broader scales.

http://www.aloki.hu ● ISSN 1589 1623 (Print) ● ISSN 1785 0037 (Online)
DOI: http://dx.doi.org/10.15666/aeer/2401_11471165

The Coupled Model Intercomparison Project (CMIP), coordinated by the Working Group on Coupled Modelling of the World Climate Research Programme, provides a unified framework for evaluating and improving climate models (Eyring et al., 2016). The project has progressed to its sixth phase (CMIP6), representing substantial advancements relative to the fifth phase (CMIP5). CMIP6 offers enhanced resolution, improved experimental designs, and a wider range of targeted experiments. It further incorporates more complex representations of physical processes (Yang et al., 2021), improves dynamic simulations (Jian et al., 2020; Zhang et al., 2019; Zhao et al., 2019; Song et al., 2021), and addresses long-standing biases identified in CMIP5 (Jian et al., 2020). As the mainstream international framework for climate simulations, CMIP6 plays a vital role in regional climate assessments and future projections. Recent studies suggest that precipitation in the Sichuan section of the Yangtze River Basin is projected to increase under multiple scenarios, with the most pronounced rise in the northwest (Chen et al., 2024). Similarly, runoff in the Jialing and Jinsha River basins is expected to increase, although drought risk in autumn and winter remains considerable (Wu et al., 2024; Zhang et al., 2023). In addition, risks from extremes—including rainstorm-induced floods and droughts—are projected to intensify, with high-risk areas concentrated in the Sichuan Basin and adjacent regions (Huang and Li, 2022; Xue et al., 2023).

As a key water source region in Sichuan Province, the Minjiang River Basin plays a crucial role in water supply, irrigation, navigation, and hydropower generation. It constitutes an integral part of the ecological barrier in the upper Yangtze River and serves as a core component of the Sichuan–Yunnan ecological barrier (Du et al., 2015). The basin's climate is highly complex, shaped by atmospheric circulation, uneven spatiotemporal precipitation, and heterogeneous topography (Wen, 2006). Droughts occur frequently and exert multiple impacts: (i) since the 1990s, declining precipitation has markedly increased drought frequency and intensity, threatening agricultural productivity and water security (Du et al., 2015); (ii) drought has long-term inhibitory effects on vegetation recovery, as shown by the slow restoration after the extreme drought of 2006, underscoring ecological vulnerability and legacy effects (Li et al., 2023); and (iii) rapid transitions between drought and flood enhance the risk of compound disasters such as landslides and debris flows (Zhang et al., 2022).

Given these challenges, selecting an appropriate drought index is critical for identifying and characterizing drought in the basin. Previous studies have primarily applied the Standardized Precipitation Index (SPI) or related metrics at a limited number of meteorological stations. For example, Du et al. (2015) reported a sharp increase in drought frequency since 1990 based on SPI analysis at 14 stations, whereas Li (2023) found particularly severe drought conditions in the upper basin. Zhou et al. (2019) employed run theory and copula functions to reveal more severe drought in the western basin, whereas Wei et al. (2024) highlighted increasing compound drought–heat events in western Sichuan using SPEI. However, most of these studies relied on roughly ten stations, limiting the ability to characterize basin-wide drought features.

To address these gaps, this study uses CN05.1 precipitation data from 249 grid points in the Minjiang River Basin (1961–2022) to analyze SPI at multiple timescales, together with drought extent and frequency. The ability of SPI to identify historical drought events is evaluated, and future drought scenarios are projected using CMIP6 model outputs. The results provide a scientific basis for drought monitoring and early warning in the Minjiang River Basin, and support enhanced regional water resource management and drought risk reduction.

http://www.aloki.hu ● ISSN 1589 1623 (Print) ● ISSN 1785 0037 (Online)
DOI: http://dx.doi.org/10.15666/aeer/2401_11471165

Data and methods

Overview of the study area

The Minjiang River Basin, a major tributary of the Yangtze River, is situated in central Sichuan Province, China. It originates in the southern foothills of the Minshan Mountains, flows through Aba, Chengdu, Meishan, and Leshan, and joins the Yangtze River at Yibin. The terrain descends gradually from west to east, and the basin covers approximately 133,500 km², as shown in *Figure 1*.

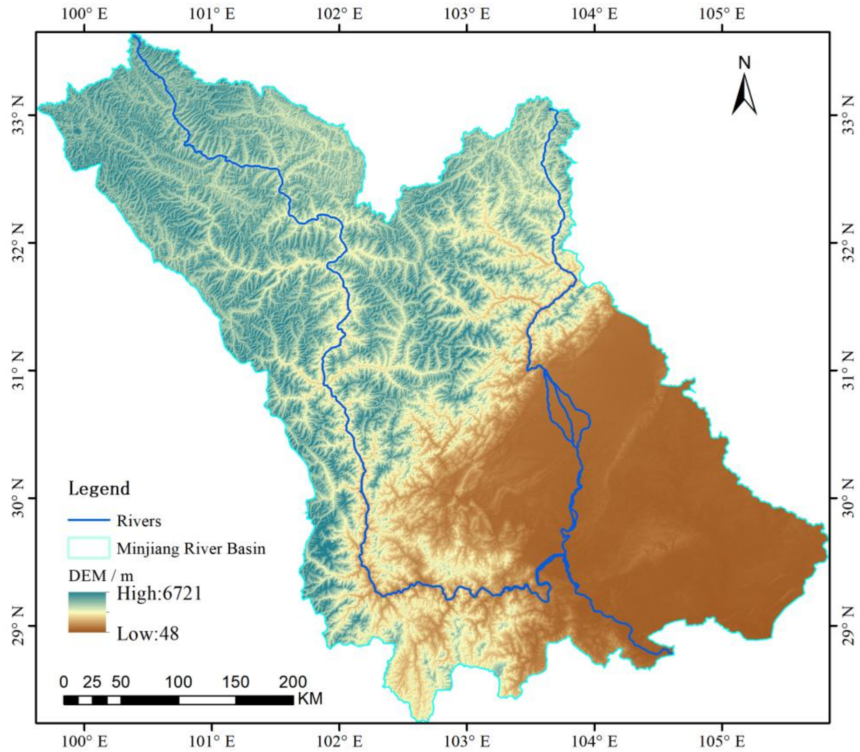

Figure 1. *Minjiang River Basin*

Data source

The observational dataset used in this study is the daily precipitation product CN05.1 (used for SPI-based climate analysis and bias correction), released by the China Meteorological Administration. The dataset is constructed through gridding and interpolation of records from more than 2400 national stations, covering 1961–2022 with a spatial resolution of 0.25° × 0.25°. It has been extensively validated and applied in studies of Southwest China and Sichuan Province (Chen et al., 2024; Xue et al., 2023; Xue and Li, 2023).

The model data are derived from CMIP6 global climate models (https://esgf-node.llnl.gov/search/cmip6). Following previous studies (Wu et al., 2024; Huang and Li, 2022; Huang et al., 2021), outputs from nine models are selected (*Table 1*), including historical simulations (1850–2014, used for bias correction) and future projections (2015–2100) under four SSP scenarios (SSP1-2.6, SSP2-4.5, SSP3-7.0, and SSP5-8.5, used only for prediction). Due to the coarse spatial resolution and inherent systematic errors of atmospheric circulation models, raw precipitation outputs often contain substantial biases.

http://www.aloki.hu ● ISSN 1589 1623 (Print) ● ISSN 1785 0037 (Online)
DOI: http://dx.doi.org/10.15666/aeer/2401_11471165

To improve the reliability and applicability of projected precipitation, bias correction was applied (Chen et al., 2024).

Table 1. *Main information of the 9 CMIP6 coupling models selected in this study*

No.	Model name	Horizontal resolution (latitude × longitude grid points)	Country/region
1	ACCESS-ESM1-5	145 × 192	Australia
2	MIROC6	128 × 256	Japan
3	EC-Earth3	256 × 512	Europe
4	GFDL-CM4	180 × 288	USA
5	MPI-ESM1-2-HR	192 × 384	Germany
6	IPSL-CM6A-LR	143 × 144	France
7	BCC-CSM2-MR	160 × 320	China
8	CanESM5	64 × 128	Canada
9	FGOAL-f3-L	180 × 360	China

Historical disaster records were mainly obtained from the General Compendium of Meteorological Disasters in China (Sichuan Volume), the China Meteorological Disaster Yearbook, the Sichuan Provincial Water Conservancy Gazetteer, and related literature (Du and He, 2015; Wang et al., 2023). Yearbook-based drought records are used as an independent reference to evaluate the performance of SPI3 and SPI12, rather than being directly combined with SPI statistics.

Methods

(1) SPI drought level classification criteria

This study applies the Standardized Precipitation Index (SPI), first proposed by McKee et al. (1993), to analyze drought characteristics in the Minjiang River Basin across multiple timescales. According to the classification criteria of the National Climate Center, drought categories are determined based on SPI thresholds (Chen et al., 2023), as summarized in *Table 2*. The SPI can be calculated over multiple timescales, each reflecting distinct physical processes. For example, SPI3, calculated over a 3-month period, reflects short-term agricultural drought conditions such as soil moisture deficits and reduced crop yields. In contrast, SPI12, based on a 12-month accumulation, captures long-term hydrological drought associated with groundwater variation, streamflow, and reservoir storage (Niu et al., 2015). In this study, SPI3 and SPI12 are applied to analyze the spatiotemporal distribution of drought in the Minjiang River Basin, and SPI12 is further employed to project future drought conditions under climate change scenarios.

Table 2. *Drought classification of the standardized precipitation index*

Level	Class	SPI
1	No drought	$-0.5 \leq SPI$
2	Mild drought	$-1.0 < SPI \leq -0.5$
3	Moderate drought	$-1.5 < SPI \leq -1.0$
4	Severe drought	$-2.0 < SPI \leq -1.5$
5	Extreme drought	$SPI \leq -2.0$

http://www.aloki.hu ● ISSN 1589 1623 (Print) ● ISSN 1785 0037 (Online)
DOI: http://dx.doi.org/10.15666/aeer/2401_11471165

(2) Drought frequency

Drought frequency is defined as the proportion of drought occurrences at grid point *i* relative to the total number of samples. It is calculated as:

$$P_i = \frac{n_i}{N_i} \quad \text{(Eq.1)}$$

where *N* denotes the total number of years with meteorological records at point *i*, and *n* represents the number of years in which drought occurred at that point.

(3) Drought scope (Chen et al., 2023)

Drought scope is defined as the proportion of grid points experiencing drought in year *j* relative to the total number of grid points in the study area, expressed as:

$$P_j = \frac{m}{M} \quad \text{(Eq.2)}$$

where *m* denotes the number of grid points experiencing drought, and *M* is the total number of grid points in the study area. The drought extent is further classified based on P_j: when $P_j \geq 50\%$, the event is identified as a region-wide drought.

(4) Bias correction

The Delta method is applied to correct systematic biases in climate model simulations. This approach has been widely adopted and proven effective in reducing discrepancies between model outputs and observations (Li et al., 2025). The correction is performed as follows:

$$P_a = P_{ow} \times \left(\frac{P_{obs}}{P_o}\right) \quad \text{(Eq.3)}$$

where P_{ow} and P_a are the precipitation values before and after bias correction, respectively; P_{obs} is the historical climatological mean of the observed precipitation data, and P_o is the historical climatological mean of the model precipitation data.

(5) Taylor diagram

The Taylor diagram provides a concise statistical framework for evaluating model performance against observations (Liu et al., 2014). Specifically, the correlation coefficient gauges the model's ability to capture temporal variability, the root-mean-square error (RMSE) quantifies deviations from observations, and the model-to-observed standard deviation ratio reflects the ability to reproduce variability amplitude. In this study, Taylor diagrams are used to evaluate each CMIP6 model, normalizing the observed standard deviation to 1 and setting the reference RMSE to 0.

Time-scale analysis

Comparison of drought identification results

Figure 2 illustrates the SPI of the Minjiang River Basin at different timescales during 1961–2022. When SPI > 0, monthly precipitation exceeds the climatological mean for the

http://www.aloki.hu ● ISSN 1589 1623 (Print) ● ISSN 1785 0037 (Online)
DOI: http://dx.doi.org/10.15666/aeer/2401_11471165

corresponding month, whereas SPI < 0 indicates drier-than-average conditions. In this study, however, drought months are defined only when SPI ≤ −0.5, following the classification in *Table 2*; months with SPI > −0.5 are regarded as non-drought conditions. SPI3 and SPI12 generally range from −3 to 3, with most value concentrated between −2 and 2. SPI behavior varies with the accumulation period: SPI3 exhibits frequent, sharp fluctuations, reflecting rapid alternations between drought and flood and better representing short-term hydro-meteorological variability. By contrast, SPI12 varies more smoothly, highlighting the periodicity of drought–flood events. This demonstrates that as the accumulation period increases, short-term features tend to be smoothed out, leading to differences in the ability of SPI to capture drought events across timescales.

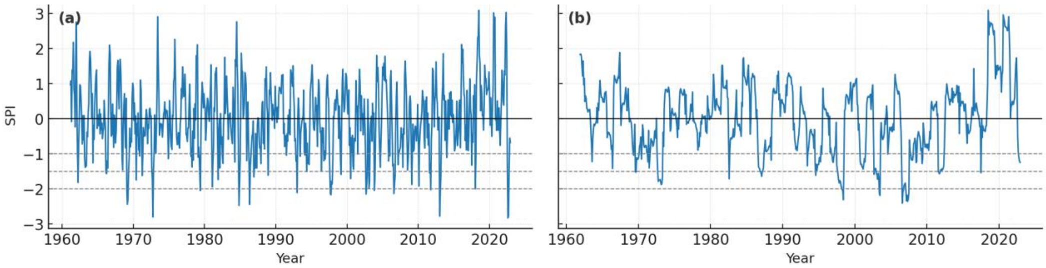

Figure 2. *Time series of SPI at different time scales: (a) SPI3; (b) SPI12*

We further analyze the persistence of SPI-identified droughts across timescales and present bar charts of event durations for SPI3 and SPI12. As shown in *Figure 3a*, the SPI3 aggregates precipitation over three-month periods (n-2, n-1, n) and is highly sensitive to short-term precipitation fluctuations. Based on this determination, long-term drought events monitored in the Minjiang River Basin include: February to October 1969 (five months of moderate or worse drought); August to December 1972 (four months of moderate or worse drought); February to July 1976; February to June 1978 (three months of moderate or worse drought); February to June 1979 (four months of moderate or worse drought); March to August 1986 (four months of moderate or worse drought); December 1986 to May 1987 (five months of moderate or worse drought); September 1992 to January 1993 (three months of moderate or worse drought); May to October 1994 (four months of moderate or worse drought); July 1997 to January 1998 (six months of moderate or worse drought); July 2000 to March 2001 (three months of moderate or worse drought); June to October 2006 (five months of moderate or worse drought); March to July 2007 (one month of moderate or worse drought); January to June 2009 (one month of moderate or worse drought); July to December 2022 (four months of moderate or worse drought). The longest drought detected by SPI3 persisted for 10 months. These findings suggest that SPI3-detected droughts can occur in any season and, under certain conditions, persist across multiple seasons. *Figure 3b* demonstrates that SPI12 (12-month accumulation) better captures long-term hydrological variability. This extended time period allows us to identify several prolonged droughts, the longest of which lasted 27 months. Moreover, consecutive severe droughts (SPI ≤ −1.5) recur more frequently, underscoring the value of SPI12 in detecting prolonged and extreme drought conditions.

Based on the Grand Dictionary of Meteorological Disasters in China (Sichuan Volume), the China Meteorological Disaster Yearbook, the Sichuan Provincial Water Conservancy Gazetteer, and other sources, we compiled typical drought events in the

http://www.aloki.hu ● ISSN 1589 1623 (Print) ● ISSN 1785 0037 (Online)
DOI: http://dx.doi.org/10.15666/aeer/2401_11471165

Minjiang River Basin for 1961-2022 and compared them with SPI3/SPI12 identifications (*Table 3*). In these reference sources, typical historical droughts in Sichuan are classified into spring drought (Occurs from March 1 to May 5), summer drought (Occurs from April 26 to July 5), and “Fu” drought (Occurs from June 26 to September 5).

Table 3. *Comparison of SPI identification of historical typical droughts at different time scales*

Year	Historical typical drought events	SPI3	SPI12
1966	Spring (Severe), Summer (Severe), Fu	Spring (Moderate)	Spring (Mild), Summer (Mild)
1969	Spring, Summer (Severe), Fu	Spring (Severe), Fu (Mild)	Spring (Moderate), Fu (Moderate)
1972	Spring, Summer, Fu (Severe)	Fu (Severe)	Fu (Moderate)
1979	Spring (Severe), Summer	Spring (Severe)	
1982	Spring (Severe), Summer (Severe), Fu	Spring (Mild), Summer (Moderate)	Summer (Mild), Fu (Mild)
1993	Spring, Summer (Severe)		Summer (Moderate), Fu (Mild)
1994	Spring, Summer (Severe), Fu (Severe)	Spring (Severe), Summer (Moderate), Fu (Moderate)	Summer (Severe), Fu (Moderate)
1997	Summer, Fu (Severe)	Summer (Mild), Fu (Extreme)	Spring (Mild), Summer (Severe), Fu (Severe)
1998	Spring (Severe)		Spring (Extreme)
2000	Spring, Summer (Severe), Fu	Spring (Mild), Summer (Moderate), Fu (Mild)	
2001	Spring (Severe), Summer (Severe), Fu (Severe)	Summer (Moderate)	
2002	Spring, Fu (Severe)	Fu (Extreme)	
2003	Spring, Summer (Severe), Fu	Summer (Mild)	Spring (Severe), Summer (Extreme)
2006	Fu (Severe)	Spring (Mild), Summer (Mild)	Spring (Mild), Summer (Severe), Fu (Severe)
2007	Spring (Severe), Summer, Fu	Spring (Mild), Summer (Moderate), Fu (Mild)	Spring (Severe), Summer (Severe), Fu (Mild)
2011	Spring, Summer, Fu (Severe)	Fu (Moderate)	Fu (Moderate)
2021	Spring (Severe), Summer (Severe)	Summer (Mild)	
2022	Summer (Severe), Fu (Severe)	Summer (Moderate), Fu (Extreme)	Fu (Mild)
Overall agreement rate of drought identification: 78.12%		**Overall agreement rate of severe drought identification: 91.0%**	

To verify the capability of SPI3 and SPI12 in identifying typical historical droughts, the time periods used in this section correspond closely to those in the Yearbook-based drought records. Subsequent sections analyze seasonal drought characteristics by spring (March–May), summer (June–July), autumn (September–November), and winter (December–February).

For the overall coincidence rate, historical droughts are classified each year into two categories—spring and summer/Fu (combined)—without distinguishing drought

http://www.aloki.hu ● ISSN 1589 1623 (Print) ● ISSN 1785 0037 (Online)
DOI: http://dx.doi.org/10.15666/aeer/2401_11471165

intensity. A historical event is counted as a 'hit' if either SPI3 or SPI12 indicates drought in the corresponding season. The overall coincidence rate equals the number of hits divided by the total number of historical events. For the severe-drought coincidence rate, only records marked 'severe' or 'extreme' are considered. Spring is counted separately, while summer and Fu seasons are combined, and the same judgment rules are applied for calculation.

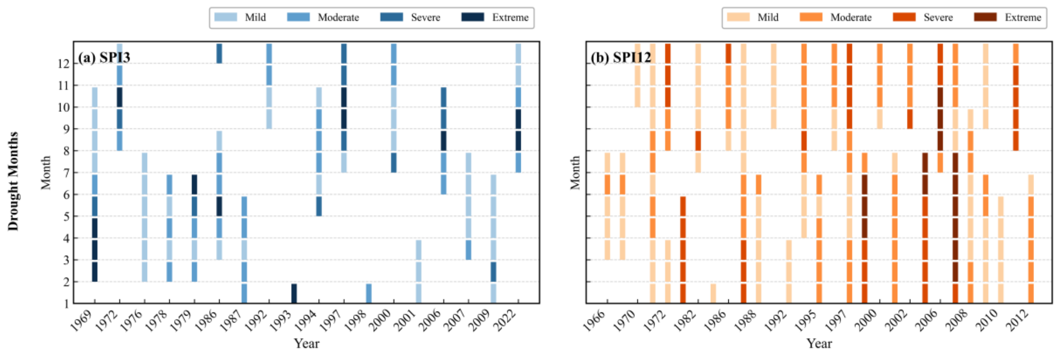

Figure 3. *Number of months of long-duration droughts identified by SPI at different time scales: (a) SPI3; (b) SPI12*

The results demonstrate that both indices capture historical drought events with reasonable accuracy. SPI3 is more sensitive to seasonal droughts, whereas SPI12 is less effective for short-term events but better suited to identifying long-term drought conditions. According to *Table 3*, when SPI3 and SPI12 are used jointly, the overall coincidence rate between historical drought events and SPI-based identification is 78.12% for all events, and 91.0% for severe and extreme events.

In summary, our results confirm that SPI3 provides a clearer representation of short-term variability, while SPI12 better characterizes periodic features at longer timescales. Consistent with the theoretical properties of the index, we observed that persistence positively correlates with the accumulation timescale, whereas sensitivity to precipitation shows an inverse correlation. Given their successful identification of typical and severe historical droughts in the Minjiang River Basin, both indices are recommended for drought monitoring and research in this region.

Interannual variation characteristics of drought

As shown in *Table 4*, drought indices in the Minjiang River Basin exhibit contrasting seasonal trends. On the annual and spring scales, the indices show upward tendencies, with linear rates of 0.01/10a and 0.2/10a, respectively. By contrast, downward trends are observed in summer (−0.04/10a), autumn (−0.06/10a), and winter (−0.007/10a). Among these, only the spring index passes the significance test, whereas the annual, summer, autumn, and winter indices do not. These results indicate that during 1961–2022 the basin experienced a weak wetting trend on the annual scale, weak drying in summer, autumn, and winter, and a relatively pronounced wetting trend in spring. On the annual scale, mild drought occurred in 1970, 1971, 1982, 1987, 1991, 2003, 2009; moderate drought occurred in 1969, 1994, 1996, 2000, 2002, 2007, 2011, 2022, while severe drought occurred in 1972, 1986, 1997, 2006; no extreme drought events were identified during the study period (*Table 5*).

http://www.aloki.hu ● ISSN 1589 1623 (Print) ● ISSN 1785 0037 (Online)
DOI: http://dx.doi.org/10.15666/aeer/2401_11471165

Table 4. *Changes in seasonal and annual scale SPI in the Minjiang River Basin*

	Year/10a	Spring/10a	Summer/10a	Autumn/10a	Winter/10a
Trend	0.01	0.2*	-0.04	-0.06	-0.007

Table 5. *Years of occurrence of drought events at different classes on the annual scale*

Drought class	Years
Mild drought	1970, 1971, 1982, 1987, 1991, 2003, 2009
Moderate drought	1969, 1994, 1996, 2000, 2002, 2007, 2011, 2022
Severe drought	1972, 1986, 1997, 2006
Extreme drought	None

Figure 4 presents temporal variations in drought scope across the basin. As shown in *Figure 4a*, basin-wide droughts at the annual scale occurred in 1969–1970, 1972, 1986–1987, 1994, 1996–1997, 2000, 2002, 2006–2007, and 2022. Among these, mild droughts dominated in eight years, whereas moderate or more severe droughts dominated in five years.

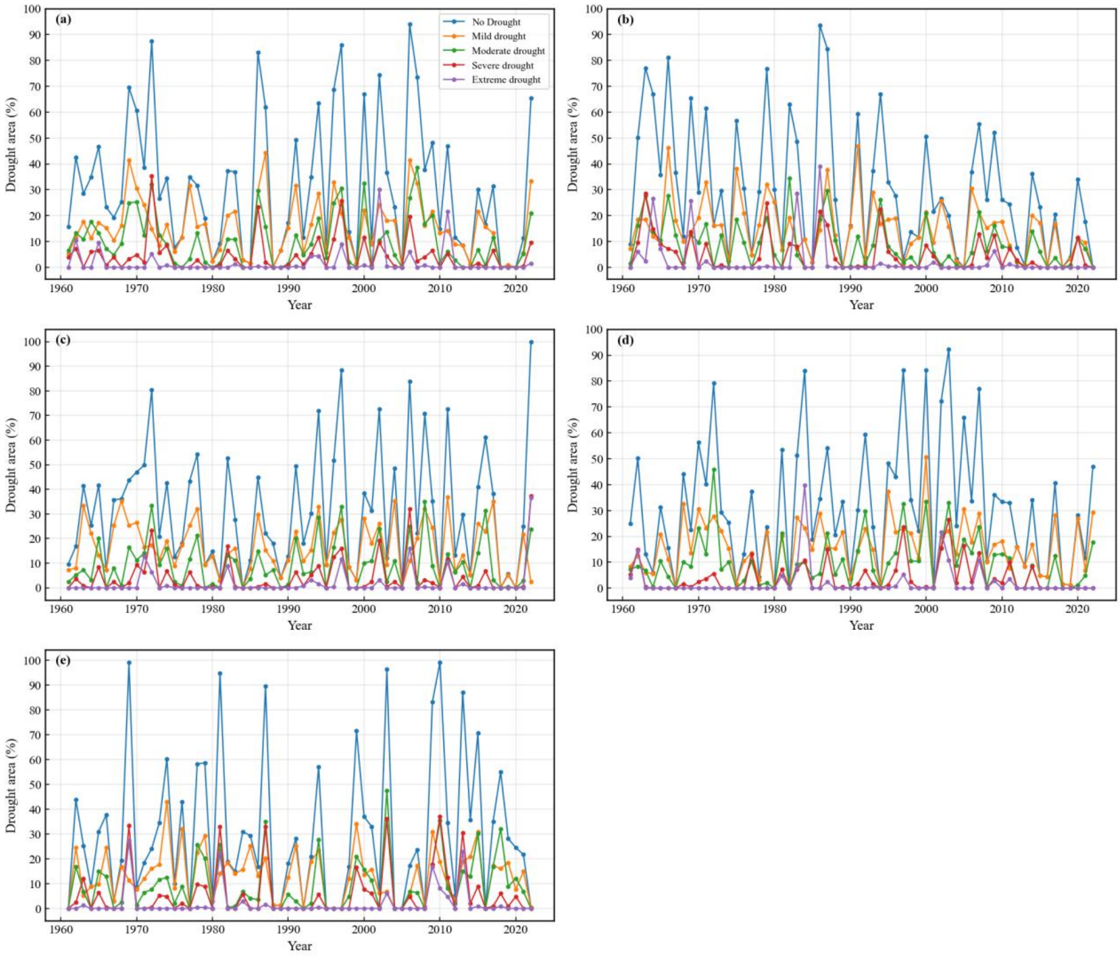

Figure 4. *Change curve of drought scope in the Minjiang River Basin. (a) Annual scale, (b) spring, (c) summer, (d) autumn, (e) winter*

http://www.aloki.hu ● ISSN 1589 1623 (Print) ● ISSN 1785 0037 (Online)
DOI: http://dx.doi.org/10.15666/aeer/2401_11471165

To avoid double counting, years identified as basin-wide annual droughts were excluded from the corresponding seasonal-scale statistics.

As shown in *Figure 4b*, basin-wide spring droughts occurred in 1962–1964, 1966, 1971, 1975, 1979, 1982, 1991, and 2009; mild droughts dominated in seven years, and moderate-or-above droughts dominated in three years.

As shown in *Figure 4c*, basin-wide summer droughts occurred in 1978, 1982, 2008, 2011, and 2016. Of these, one year was dominated by mild drought, whereas four years were dominated by moderate-or-above drought.

As illustrated in *Figure 4d*, basin-wide autumn droughts were recorded in 1962, 1981, 1983–1984, 1992, 2003, and 2005. Among these, two years were dominated by mild drought and five by moderate-or-above drought.

As illustrated in *Figure 4e*, basin-wide winter droughts occurred in 1974, 1978–1979, 1981, 1999, 2003, 2009–2010, 2013, 2015, and 2018. Mild drought dominated in five of these years, whereas six years were dominated by moderate-or-above drought.

Overall, droughts in the basin exhibited marked seasonal variability. Annual and spring droughts were generally associated with mild conditions, while summer, autumn, and winter were more often dominated by moderate-or-above drought.

Spatial scale analysis based on seasonal distribution

As illustrated in *Figure 5a*, the spatial pattern of spring drought frequency appears fairly uniform. High-value areas are concentrated in parts of Chengdu and Guoluo, with frequencies of 36–40%, highlighting priority areas for spring drought mitigation. Low-value areas occur mainly in parts of Aba and Ganzi, at 20–25%.

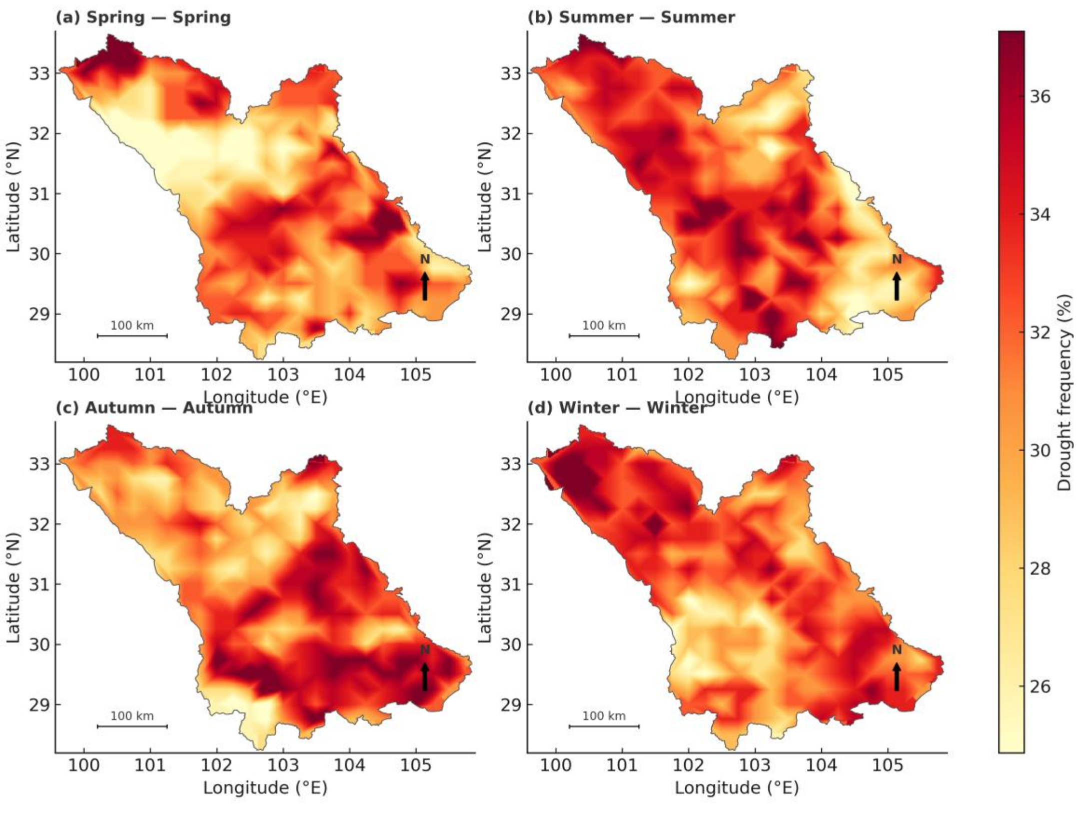

Figure 5. *Drought frequency distribution in the Minjiang River Basin*

http://www.aloki.hu ● ISSN 1589 1623 (Print) ● ISSN 1785 0037 (Online)
DOI: http://dx.doi.org/10.15666/aeer/2401_11471165

As illustrated in *Figure 5b*, the spatial distribution of summer drought frequency exhibits a pattern of 'low in the southeast and high in the northwest.' Areas of relatively high frequency (35–40%) are concentrated in Leshan, Ya'an, Guoluo, Aba, and Ganzi. In contrast, low-frequency zones are identified in Yibin and Zigong, where values range from 21% to 25%.

As shown in *Figure 5c*, the spatial distribution of autumn drought frequency exhibits a southeast-high/northwest-low pattern. High-value areas include Ya'an, Leshan, Zigong, Neijiang, and Chengdu, at 34–41%. Low-value areas occur mainly in Aba and Liangshan, at 22–26%.

As shown in *Figure 5d*, the spatial distribution of winter drought frequency presents a pattern of 'low in the northeast and southwest, but high in the northwest and southeast.' High-value areas are concentrated in parts of Guoluo, with frequencies of 36–40%. Low-value areas occur mainly in Ganzi, at 24–27%.

Seasonal drought frequencies in the Minjiang River Basin are 30.6% in spring, 32.0% in summer, 31.9% in autumn, and 32.1% in winter. As shown in *Table 6*, frequencies across all seasons follow the order mild > moderate > severe > extreme. Specifically, mild drought occurs most frequently in summer (16.4%), moderate drought peaks in autumn (10.0%), severe drought occurs most often in winter (5.7%), and extreme drought reaches its maximum in spring (2.4%). These results indicate that mild drought is the most common type in the basin, with a seasonal tendency toward summer occurrence, whereas severe and extreme droughts are more likely in spring and winter.

Table 6. *Frequencies of droughts at different levels*

Level	Frequency			
	Spring	**Summer**	**Autumn**	**Winter**
Mild drought	14.90%	16.40%	16.10%	13.20%
Moderate drought	8.60%	9.50%	10.00%	9.70%
Severe drought	4.60%	4.30%	3.80%	5.70%
Extreme drought	2.40%	1.90%	2.10%	1.90%

Evaluation and projection of the CMIP6 models

Evaluation of the CMIP6 models

As illustrated in *Figure 6*, among the nine bias-corrected models evaluated, the top three by TSS are ACCESS-ESM1-5, MIROC6, and EC-Earth3. Most models show strong correlations with observations ($R > 0.85$). ACCESS-ESM1-5 ($R = 0.94$), MIROC6 ($R = 0.92$), and EC-Earth3 ($R = 0.91$) perform best, indicating their ability to accurately capture the interannual fluctuations of precipitation. For the standard deviation ratio (SDR), most models are close to unity; ACCESS-ESM1-5 ($SDR = 0.98$), MIROC6 ($SDR = 1.00$), and EC-Earth3 ($SDR = 1.02$) show the closest agreement with observations, suggesting effective reproduction of precipitation variability. In terms of root-mean-square error (RMSE), ACCESS-ESM1-5, MIROC6, and EC-Earth3 again demonstrate superior performance, with values of 0.36–0.42, supporting their reliability in representing precipitation extremes. Therefore, a bias-corrected multi-model ensemble (r-MME) based on these three models is constructed and applied to project future drought characteristics.

http://www.aloki.hu ● ISSN 1589 1623 (Print) ● ISSN 1785 0037 (Online)
DOI: http://dx.doi.org/10.15666/aeer/2401_11471165

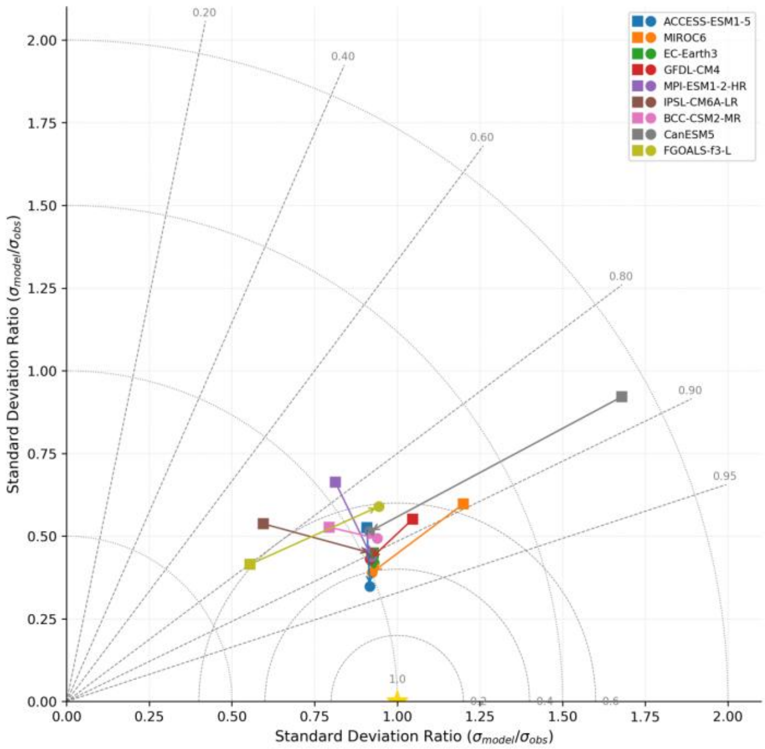

Figure 6. *Taylor diagrams comparing simulated and observed precipitation before (squares) and after (circles) bias correction for each model*

Projections of drought characteristics in the Minjiang River Basin under future scenarios

Based on the bias-corrected r-MME under SSP1-2.6, SSP2-4.5, SSP3-7.0, and SSP5-8.5, future drought characteristics in the Minjiang River Basin are evaluated with the 12-month SPI (SPI12). *Figure 7* presents the interannual variability of SPI12 across the four emission scenarios. The results show that SPI12 follows an overall upward trend in all four scenarios, with linear rates of 0.280/10a (SSP1-2.6), 0.297/10a (SSP2-4.5), 0.117/10a (SSP3-7.0), and 0.270/10a (SSP5-8.5). Except for SSP3-7.0, all trends are statistically significant, indicating that the Minjiang River Basin is likely to become wetter under most scenarios.

Further statistics on drought-event frequency, mean duration, and the occurrence of severe and extreme events (*Table 7*) reveal distinct characteristics across emission scenarios. Under SSP1-2.6, droughts are relatively frequent and long-lasting but have a low likelihood of intensifying to severe or extreme levels. Under SSP2-4.5, droughts are frequent and prone to intensify into severe or extreme events. Under SSP3-7.0, droughts occur very frequently but are generally shorter in duration. By contrast, under SSP5-8.5, droughts are frequent and tend to evolve into long-lasting, high-intensity extreme events.

Figure 8 presents the temporal evolution of December drought extent—expressed as the percentage of grid points with SPI12 < −0.5—under four future emission scenarios (SSP1-2.6, SSP2-4.5, SSP3-7.0, SSP5-8.5) for 2015–2100. Across all scenarios, drought extent exhibits pronounced year-to-year fluctuations, reflecting the large interannual variability of regional hydro-climatic conditions. Despite this short-term variability, a consistent and statistically significant long-term decreasing trend is observed.

http://www.aloki.hu ● ISSN 1589 1623 (Print) ● ISSN 1785 0037 (Online)
DOI: http://dx.doi.org/10.15666/aeer/2401_11471165

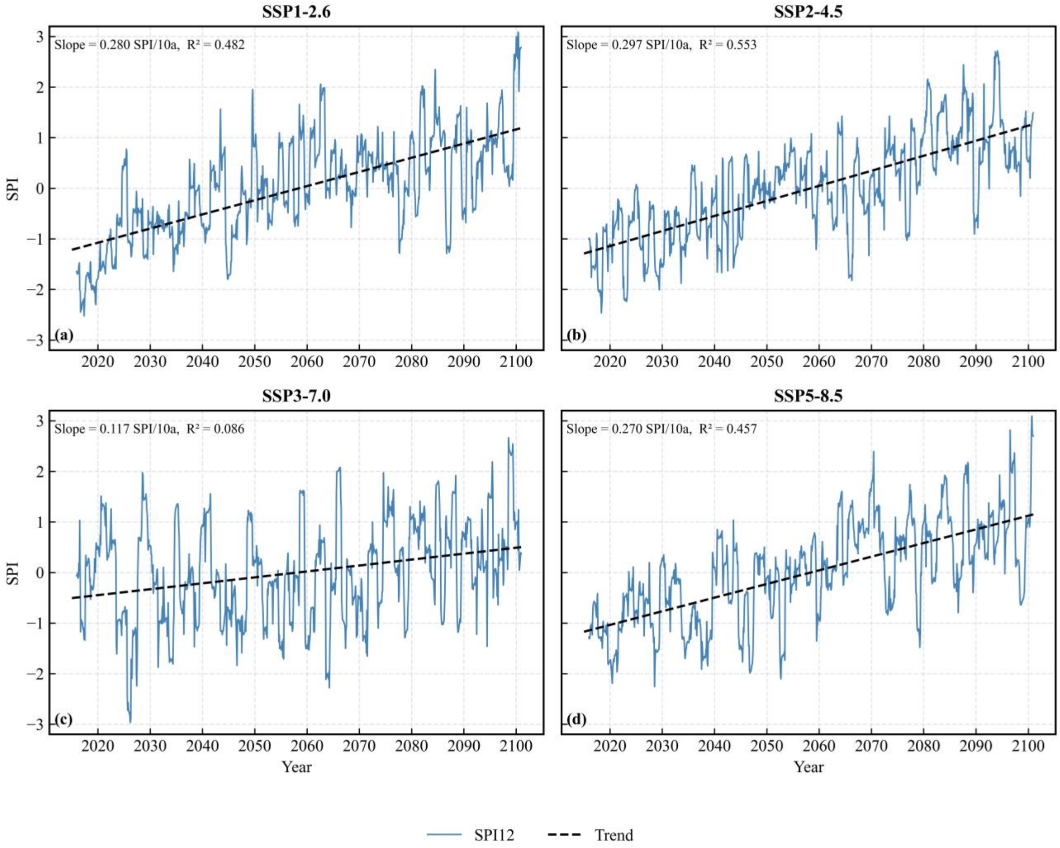

Figure 7. *Interannual variation characteristics of SPI12 for the period 2015–2100 under each emission scenario. (a) SSP1-2.6, (b) SSP2-4.5, (c) SSP3-7.0, (d) SSP5-8.5*

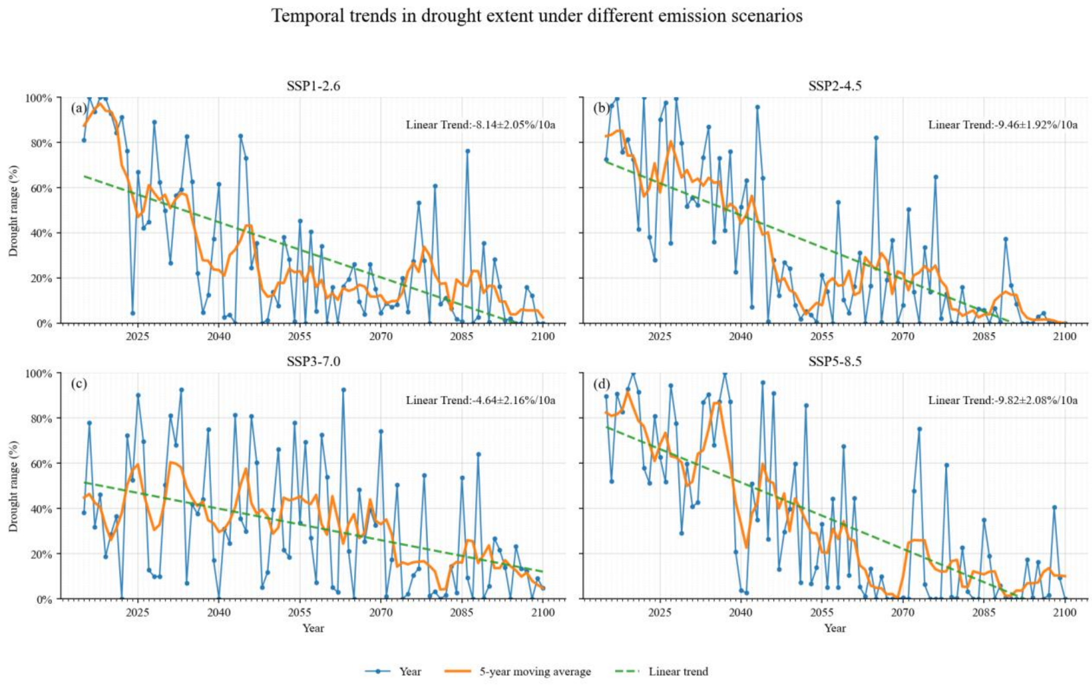

Figure 8. *Interannual variation characteristics of drought scope during 2015–2100 under each emission scenario. (a) SSP1-2.6, (b) SSP2-4.5, (c) SSP3-7.0, (d) SSP5-8.5*

http://www.aloki.hu ● ISSN 1589 1623 (Print) ● ISSN 1785 0037 (Online)
DOI: http://dx.doi.org/10.15666/aeer/2401_11471165

Table 7. *Drought characteristics in the Minjiang River Basin under different emission scenarios*

SSP scenario	Frequency of drought events	Average duration (month)	Number of severe/extreme drought events
SSP1-2.6	17	18.29	3
SSP2-4.5	18	17.89	9
SSP3-7.0	28	12.00	7
SSP5-8.5	17	19.06	7

Linear trend analysis indicates declines of –8.14 ± 2.05%/decade for SSP1-2.6, –9.46 ± 1.92%/decade for SSP2-4.5, –4.64 ± 2.16%/decade for SSP3-7.0, and –9.82 ± 2.08%/decade for SSP5-8.5. The strongest decline occurs in the highest-emission pathway SSP5-8.5, while the weakest reduction is associated with SSP3-7.0. The 5-year moving averages emphasize the downward tendencies, demonstrating that the decrease in drought coverage is robust to short-term climate variability.

These results indicate that December drought coverage is projected to shrink substantially across all scenarios, suggesting a general alleviation of widespread moderate drought in the region. However, the persistence of large interannual variability implies that severe droughts may still occur in individual years, even under scenarios with strong long-term declines. This underscores the importance of considering both long-term climate projections and short-term variability in drought risk assessments.

Figure 9 presents the spatial distribution of drought frequency derived from historical observations and projected under different emission scenarios. As shown in *Figure 9a*, observed drought frequency ranges from 0.27-0.35, exhibiting a central-high/east–west-low pattern, indicating that the central and southern regions have historically been more drought-prone.

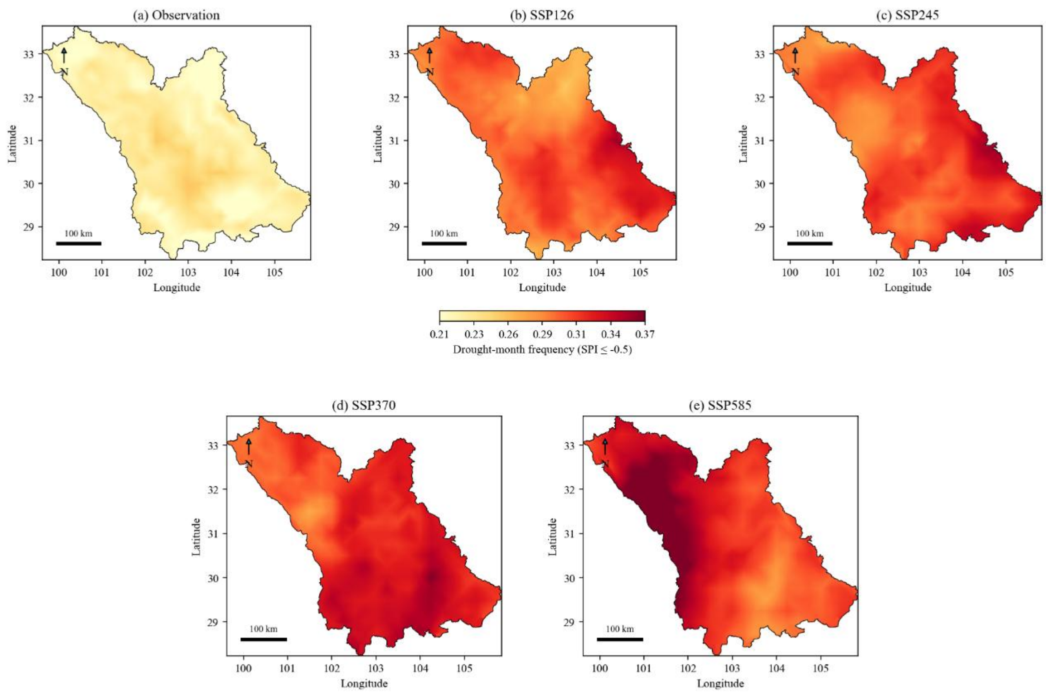

Figure 9. *Distributions of observed drought frequencies and those for 2015–2100 under various emission scenarios. (a) Observation, (b) SSP1-2.6, (c) SSP2-4.5, (d) SSP3-7.0, (e) SSP5-8.5*

http://www.aloki.hu ● ISSN 1589 1623 (Print) ● ISSN 1785 0037 (Online)
DOI: http://dx.doi.org/10.15666/aeer/2401_11471165

Under the SSP1-2.6 scenario *(Fig. 9b*), drought frequencies decrease to 0.27–0.31, particularly in the northwestern and central regions, suggesting a potential alleviation of drought risk. By contrast, SSP2-4.5 *(Fig. 9c)* shows higher frequencies, exceeding 0.34 in the southeast, indicating an intensification of drought risk there. SSP3-7.0 (*Fig. 9d*) further increases frequency, with values of 0.33–0.36 concentrated in the southern and central–eastern regions. Under SSP5-8.5 (*Fig. 9e*), drought frequency reaches its maximum, with extensive high-value centers (>0.37) in the northwest and central basin, markedly exceeding historical levels. These results suggest that the drought frequency in the Minjiang River Basin is projected to intensify substantially under higher-emission scenarios, with high-risk zones expanding markedly.

Conclusion

This study reveals the spatiotemporal characteristics and future projections of drought in the Minjiang River Basin by combining SPI indices with bias-corrected CMIP6 models. Results show that SPI3 and SPI12 effectively capture short- and long-term drought variability, with high recognition accuracy for historical events. The basin exhibits a weak annual wetting trend with marked seasonal differences; drought occurs in all seasons with notable spatial hotspots. Future drought characteristics differ across SSP scenarios, with intensity and frequency generally increasing under higher-emission pathways. These findings provide a scientific basis for drought monitoring and risk management in the region.

1. SPI3 effectively represents short-term drought–flood variability, whereas SPI12 better captures the periodic variability of droughts and floods. When SPI3 and SPI12 are used jointly, the overall coincidence rate for historical typical droughts reaches 78.12%, and the coincidence rate for severe and extreme droughts reaches 91.0%. Both indices are suitable for drought identification and research in the Minjiang River Basin.

2. On an annual scale, the Minjiang River Basin shows a weak wetting trend (0.01/10a). In spring, it exhibits a relatively significant wetting trend (0.2/10a), while in summer (-0.04/10a), autumn (-0.06/10a), and winter (-0.007/10a), there are weak drying trends.

3. Regional droughts occur in all four seasons. In spring they are mainly dominated by mild drought, whereas in summer, autumn, and winter they are largely dominated by moderate-or-above drought. Seasonal extreme regional droughts are often accompanied by severe and extreme drought.

4. Consistent with general drought climatology, mild events constitute the most frequent drought category in the basin, followed by moderate, severe, and extreme events. In the Minjiang River Basin, mild droughts occur most often in summer, whereas severe and extreme droughts are more likely in spring and winter. Spatially, high-value areas are located in parts of Chengdu and Guoluo in spring; Leshan, Ya'an, Guoluo, Aba, and Ganzi in summer; Ya'an, Leshan, Zigong, Neijiang, and Chengdu in autumn; and Guoluo in winter. These hotspots should be prioritized for seasonal drought prevention and mitigation.

5. The bias-corrected CMIP6 models accurately reproduce interannual variability, precipitation variability, and precipitation extremes. Among them, ACCESS-ESM1-5, MIROC6, and EC-Earth3 perform particularly well. Accordingly, a calibrated multi-model ensemble (r-MME) based on these three models can be used to project drought characteristics.

http://www.aloki.hu ● ISSN 1589 1623 (Print) ● ISSN 1785 0037 (Online)
DOI: http://dx.doi.org/10.15666/aeer/2401_11471165

6. Under future scenarios, drought characteristics differ: under SSP5-8.5, droughts exhibit low frequency, long duration, and high intensity; under SSP3-7.0, high frequency and short duration; under SSP2-4.5, frequency and duration lie between SSP5-8.5 and SSP3-7.0 but with relatively high intensity; under SSP1-2.6, low frequency, long duration, and low intensity. Meanwhile, the drought-affected area is projected to decline. Spatially, drought frequency increases progressively from SSP1-2.6 → SSP2-4.5 → SSP3-7.0 → SSP5-8.5. High-value areas extend from the central basin (observation period) to the southeast and south, and then to the northwest and central basin. Greater attention should therefore be paid to drought-risk management in the southern, central, and northwestern regions.

Discussion

(1) Consistency with and contributions to existing regional studies

An SPI–copula analysis for the upper Minjiang River (Qin et al., 2021) reported more severe drought risk in the western basin, broadly consistent with this study's identification of central–adjacent high-value areas under high-emission scenarios. Using higher-density grid data (CN05.1) and the full CMIP6 scenario set, this study offers advantages in resolving spatial detail and characterizing future evolution. The record-breaking compound heatwave–drought event in the region caused significant impacts on energy–water systems and the environment. This study identifies the extreme regional drought in 2022 (the affected area in summer reached 100%) on the summer and annual scales, which is basically consistent with the historical records of that year. These findings underscore the need to incorporate heat–drought compounding into drought identification and assessment (Chen et al., 2024; Seneviratne et al., 2021).

(2) Coexistence of "wetter mean" and "more dangerous extremes"

Multiple CMIP6-based studies for China and Southwest China indicate that, even as annual or cold-season mean moisture becomes wetter, drought-event frequency, duration, and intensity do not change monotonically. Some regions exhibit a structural change—decreasing event frequency but increasing intensity and/or duration—consistent with our finding that SSP5-8.5 yields longer, stronger droughts, whereas SSP3-7.0 yields more frequent but shorter events (Seneviratne et al., 2021; Miao et al., 2024).

(3) Uncertainties in model capabilities and bias correction

CMIP6 evaluations for China generally indicate that, relative to temperature, the spatial distribution and interannual variability of precipitation are harder to simulate. Appropriate bias correction can markedly improve distributional properties and correlations, but different methods affect extreme quantiles and drought indices (SPI/SPEI) to varying degrees. In this study, the delta method yields positive improvements, consistent with evaluations at national and regional scales. Nevertheless, caution is warranted for behavior in the distribution tails (Rajulapati et al., 2023).

(4) Selection of indicators and scales

The Standardized Precipitation Index (SPI) is highly sensitive to precipitation anomalies, and the differing sensitivities of SPI3 and SPI12 are clearly evidenced in this

http://www.aloki.hu ● ISSN 1589 1623 (Print) ● ISSN 1785 0037 (Online)
DOI: http://dx.doi.org/10.15666/aeer/2401_11471165

study. However, under compound extremes (e.g., heat–drought–wind), a single SPI may underestimate the drought impacts of “heat-induced pressurization.” Recent studies on compound drought events (CDHE/HDWE) show that, against a backdrop of rising temperatures, increasing synchrony, persistence, and concurrent intensity of heatwaves and droughts constitute a key pathway explaining the phenomenon of “wetter on average but more dangerous in extremes.” In future work, the Standardized Precipitation–Evapotranspiration Index (SPEI), evapotranspiration-based indicators, or compound indices will be introduced for sensitivity comparisons (Seneviratne et al., 2021; Miao et al., 2024).

(5) Managerial implications

Against the backdrop of the coexistence of “narrowing scope and intensifying intensity (lengthening duration)”, watershed management needs to transform from “average conditions” to “extreme resilience”. On the one hand, priority should be given to deploying redundancy for drought risk in the key areas identified here (northwest–central regions under high-emission scenarios). On the other hand, for seasons prone to severe–extreme drought, interdepartmental linkage plans for electricity–water–agriculture and early warnings for compound extremes should be strengthened (Chen et al., 2024; Seneviratne et al., 2021).

Acknowledgments. This research was supported by the Joint Funds of the National Natural Science Foundation of China (U2133209), the Fundamental Research Funds for the Central Universities (25CAFUC01005, 24CAFUC03033), and the Short-Term, High-Efficiency Research Project of Chengdu Meteorological Bureau (No. 2024-1 (11)).

REFERENCES

[1] Chen, D., Qiao, S., Yang, J., Tang, S., Zuo, D., Feng, G. (2024a): Contribution of anthropogenic influence to the 2022-like Yangtze River valley compound heatwave and drought event. – NPJ Climate and Atmospheric Science 7: 172.

[2] Chen, Y., Han, Y., Sun, M., Han, L. (2024b): Prediction and analysis of future precipitation changes in the Sichuan section of the Yangtze River Basin based on CMIP6 climate models. – Research of Soil and Water Conservation 31(5): 288-294.

[3] Chen, Z., Li, J., Xiang, B., Duan, Q., Li, S., Wang, S. (2023): Spatiotemporal variation of drought in Yunnan Province calculated using the standardized precipitation index. – Journal of Irrigation and Drainage 42(4): 92-99.

[4] Du, H., He, S. (2015): Characteristics of precipitation and trends in drought and flood disasters in the Minjiang River Basin. – Research of Soil and Water Conservation 22(1): 153-157.

[5] Eyring, V., Bony, S., Meehl, G. A., Senior, C. A., Stevens, B., Stouffer, R. J., Taylor, K. E. (2016): Overview of the Coupled Model Intercomparison Project Phase 6 (CMIP6) experimental design and organization. – Geoscientific Model Development 9(5): 1937-1958.

[6] Huang, X., Li, X. (2022): Future projection of rainstorm and flood disaster risk in Southwest China based on CMIP6 models. – Journal of Applied Meteorological Science 33(2): 231-243.

[7] Huang, Z., Wu, X., Mao, J. (2021): An evaluation for impacts of the horizontal resolution of CMIP6 models on simulating extreme summer rainfall over Southwest China. – Plateau Meteorology 40(6): 1470-1483.

[8] Jian, B., Li, J., Zhao, Y., He, Y., Wang, J., Huang, J. (2020): Evaluation of the CMIP6 planetary albedo climatology using satellite observations. – Climate Dynamics 54(11-12): 5145-5161.
[9] Li, T. (2023): Characteristics of vegetation change and its response to drought in the Minjiang River Basin. – Master's thesis, Hubei University.
[10] Li, X., Zhu, F. (2025): Forecast and trend analysis of water demand in Guizhou Province based on CNN–LSTM. – Pearl River [online]. https://link.cnki.net/urlid/44.1037.tv.20250723.1331.002 (accessed 2025-09-06).
[11] Liu, Y., Li, W., Zuo, J., Hu, Z.-Z. (2014): Simulations and projections of the western Pacific subtropical high in CMIP5 models. – Acta Meteorologica Sinica 72(2): 277-290.
[12] McKee, T. B., Doesken, N. J., Kleist, J. (1993): The relationship of drought frequency and duration to time scales. – In: Proceedings of the 8th Conference on Applied Climatology, American Meteorological Society, Anaheim, CA, 17-22 Jan 1993, pp. 179-184.
[13] Miao, L., Ju, L., Liu, Q. (2024): Unveiling the dynamics of sequential extreme precipitation–heatwave compound events in China (1975-2020). – NPJ Climate and Atmospheric Science 7: 67.
[14] Niu, Y., Wang, S. (2015): Temporal and spatial characteristics of drought based on the standardized precipitation index in the Yellow River Basin. – Journal of Irrigation and Drainage 34(4): 85-90.
[15] Qin, F., Ao, T., Chen, T. (2021): Bivariate frequency of meteorological drought in the Upper Minjiang River based on copula function. – Water 13(15): 2056.
[16] Rajulapati, C. R., Papalexiou, S. M. (2023): Precipitation bias correction: a novel semi-parametric quantile mapping method. – Earth and Space Science 10(4): e2023EA002823.
[17] Seneviratne, S. I., Zhang, X., Adnan, M., Badi, W., Dereczynski, C., Di Luca, A., Ghosh, S., Iskandar, I., Kossin, J., Lewis, S., Otto, F., Pinto, I., Satoh, M., Vicente-Serrano, S. M., Wehner, M., Zhou, B. (2021): Chapter 11: Weather and Climate Extreme Events in a Changing Climate. – In: IPCC (ed.) Climate Change 2021: The Physical Science Basis. Cambridge University Press, Cambridge, pp. 1513-1766.
[18] Song, Z., Xia, J., She, D., Li, L., Hu, C., Hong, S. (2021): Assessment of meteorological drought change in the 21st century based on CMIP6 multi-model ensemble projections over mainland China. – Journal of Hydrology 601: 126643.
[19] Wang, J., Li, W., Li, C., Dong, Y., Zhao, G., Xu, T., Li, Z. (2021): Drought characteristics in Ningxia based on standardized precipitation index. – South-to-North Water Transfers and Water Science & Technology 19: 528-538.
[20] Wang, Y., Lan, L., Lei, S., Wang, X., Wang, X. (2023): Study on spatial-and-temporal characteristics of typical drought events in Sichuan Province. – China Flood & Drought Management 33(4): 22-26.
[21] Wei, R., Pan, N., Zhong, X., Zhao, L., Liang, C., Cui, N. (2024): Variation characteristics of extreme high-temperature and drought compound events in Sichuan Province. – Journal of China Hydrology 44(6): 60-67.
[22] Wen, K. (ed.) (2006): China Meteorological Disasters Canon: Sichuan Volume. – China Meteorological Press, Beijing.
[23] Wu, M., Ni, F., Deng, Y., Yue, Z., Jiang, N., Kang, W., Xiang, J. (2024): Projections of runoff and hydrological drought in the Jialing River Basin based on CMIP6. – Resources and Environment in the Yangtze Basin 33(5): 1004-1017.
[24] Xue, S., Li, X. (2023): Analysis of spatial and temporal distribution characteristics of summer precipitation in Sichuan in the past 40 years. – Science Technology and Industry 23(22): 246-252.
[25] Xue, Y., Li, X., Jia, H. (2023): Future projection of drought risk in Southwestern China based on CMIP6 models. – Research of Soil and Water Conservation 30(2): 247-255.
[26] Yang, X., Zhou, B., Xu, Y., Han, Z. (2021): CMIP6 evaluation and projection of temperature and precipitation over China. – Advances in Atmospheric Sciences 38(5): 817-830.

[27] Yin, H., Bai, F. (2025): Study on the spatiotemporal evolution and driving forces of meteorological drought in the Yellow River Basin considering spatial heterogeneity. – China Rural Water and Hydropower 2025(2): 74-80.
[28] Zhai, P., Zou, X. (2005): Changes in temperature and precipitation and their impacts on drought in China during 1951-2003. – Advances in Climate Change Research 1(1): 15-18.
[29] Zhang, D., Liang, H., He, X., Shi, Y. (2023): Estimation of runoff and hydrological drought in the Jinsha River Basin based on CMIP6. – Water Resources Protection 39(6): 53-62.
[30] Zhang, L., Zhou, J., Zhang, H., Wang, B., Cao, J. (2017): Temporal and spatial patterns of climate wetness–dryness and drought events based on the standardized precipitation index in the Shiyang River Basin. – Acta Ecologica Sinica 37(3): 996-1007.
[31] Zhang, L., Chen, X., Xin, X. (2019): ScenarioMIP in CMIP6: overview and comments. – Advances in Climate Change Research 15(5): 519-525.
[32] Zhang, X., Xu, X., Li, X. (2022): Changes of abnormal precipitation with warming in the Minjiang River Basin in the past 40 years. – Journal of Natural Disasters 31(4): 44-56.
[33] Zhao, Y., Xiao, D., Bai, H. (2019): Projection and application for future climate in China by CMIP5 climate models. – Meteorological Science and Technology 47(4): 608-621.

http://www.aloki.hu ● ISSN 1589 1623 (Print) ● ISSN 1785 0037 (Online)
DOI: http://dx.doi.org/10.15666/aeer/2401_11471165